Revue des Composites et des Matériaux Avancés-Journal of Composite and Advanced Materials
Vol. 35, No. 1, February, 2025, pp. 81-86
Journal homepage: http://iieta.org/journals/rcma

Effect of Hot Water Treatment Time on the Structure and Optical Properties of ZnO Nanostructures

Iman Hamza Irhayem[1], Khalidah H. Al-Mayalee[2*]

[1] General Directorate of Muthanna Education, Al Muthanna 66001, Iraq
[2] Department of Physics, Faculty of Education for Women, University of Kufa, Najaf 54001, Iraq

Corresponding Author Email: khalidah.almayali@uokufa.edu.iq

https://doi.org/10.18280/rcma.350110

Received: 21 January 2025
Revised: 16 February 2025
Accepted: 22 February 2025
Available online: 28 February 2025

Keywords:
ZnO nanostructures, hot water treatment method, deposition time, morphological properties, optical properties

ABSTRACT

ZnO nanorod structures were deposited on glass substrates using varying deposition times utilizing an easy hot water treatment technique. Thin zinc films have been grown on glass substrates by the thermal physical vapor deposition technique, and the samples were then oxidized with hot water at 75°C for 10, 20, 30 minutes. Using field emission scanning electron microscopy (FESEM) and X-ray diffraction (XRD), the shape and structure of the as-prepared samples were examined. Results showed that the ZnO films are polycrystalline and in the hexagonal wurtzite phase, and the samples showed the uniform thin film with nanorod-like nanocrystalline morphology. The optical characteristics of the as-grown ZnO nanostructures at different growth times have been studied using UV-Vis spectroscopy technique. The influence of hot water treatment time on the optical properties was reported and discussed. Results showed that the optical transmittance in the visible area was around 95%, 90%, and 48% at 10 min, 20 min, and 30 min, respectively. The optical energy gap of the ZnO nanostructure samples varied from 3.46 eV to 3.32 eV when the preparation time was extended from 10 to 30 minutes. According to the findings, high-quality ZnO nanorods can be formed when deposited at a growth time of 30 minutes.

1. INTRODUCTION

Zinc oxide (ZnO) nanostructures are being an important transition metal oxides in different applications due to their excellent electrical, mechanical, optical, and thermal properties [1, 2]. In the visible and infrared spectrums, ZnO, an n-type semiconductor, has great optical transparency, a direct wide band gap (Eg = 3.37 eV), higher exciton binding energy, and high chemical stability [3-5]. It is also an abundant, inexpensive, environmentally friendly and nontoxic material [5, 6]. There are several uses of ZnO nanomaterials in electronics and photonics, such as light-emitting diodes, liquid crystal displays, solar cells, gas sensing devices, and thermal mirrors [6-9].

ZnO films have been synthesized using a variety of techniques, including pulsed laser deposition [3], sputtering using RF/DC magnetrons [4], chemical bath deposition [5], vacuum evaporation using reactive heat [6], sol-gel technique [7], and spray pyrolysis [8, 9]. In this work, the hot water treatment (HWT) approach was used to develop zinc oxide films on glass substrates. HWT is a potentially more economical, clean, efficient, and easy method to create metal oxides easily on numerous substrates. A wide range of metals have been treated by HWT method to produce metal oxides such as Al_2O_3, CuO, Cu_2O), Fe_2O_3, MgO, TiO_2, and ZnO [10-14]. Without the need for catalysis during the synthesis of NSs, the HWT approach has the useful benefits of high-throughput manufacturing and flexibility to a broad variety of materials having boiling points higher than water [10, 12].

The structural features of the nanostructured materials will be examined in this work using X-ray diffraction (XRD), the surface morphology will be examined using FE-SEM, and the optical properties will be examined using UV spectroscopy.

2. EXPERIMENTAL PROCEDURE

Zinc (Zn) powder with an atomic density of 7.133 g/cm^3, a molecular weight of 65.39 g/mol, and high purity (99.9%) was purchased from the local market and used to produce a 300 nm-thick Zn metal thin film on clean glass substrates via the thermal evaporation technique.

The glass substrates (2 cm × 2 cm) were cleaned using ultrasonication in acetone and deionized water for 5 minutes each, followed by air drying. The cleaned substrates were then placed on a ceramic holder inside the deposition chamber at room temperature. The evaporation process commenced once the base pressure reached 5 × 10^{-7} mbar. The deposition rate was maintained at 10 nm/s, with the voltage set at 150 kV.

To synthesize ZnO nanostructures (NSs), the as-prepared Zn thin films on glass substrates were immersed in a clean beaker containing 200 ml of deionized water with a pH of

approximately 7. The solution was maintained at a constant temperature of 75°C using a thermostat (temperature-control rod) for varying immersion durations (10, 20, and 30 minutes). Finally, the samples were air-dried for 5 hours.

Following deposition, the films were characterized using scanning electron microscopy (SEM) and X-ray diffraction (XRD). The detailed fabrication process of ZnO nanostructures on glass substrates is illustrated in Figure 1.

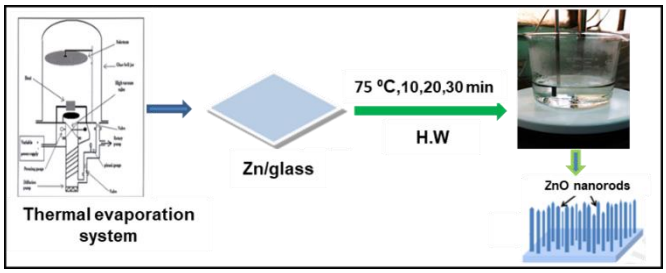

Figure 1. Schematic of ZnO fabrication on a glass substrate

3. RESULTS AND DISCUSSION

3.1 Morphological analysis

A typical Images from SEM of the prepared structures is shown in Figure 2. The photos reveales the development of dense, vertically aligned nanorod morphologies with different diameters of ZnO nanostructures (NSs) on glass substrate surface. Figure 2(a) shows the ZnO NSs after 10 minutes of immersing Zn thin film in hot dionized water at 75°C. Image presents the nucleation and growth of ZnO nanorod-like structures on glass substrate. After 20 min of hot water treatment, the nanorods condensed into rod-like formations and all of the nanorods were perpendicular to the substrate and some voids appeared between them (Figure 2(b)). As can be seen in Figure 2(c), well-aligned ZnO nanorod arrays with longer and greater diameters were formed on ITO substrate after 30 min of synthesis time and the nanorods have hexagonal pointed tips. The ZnO nanorod structures were in accordance with previous results reported by Saadi et al. [10].

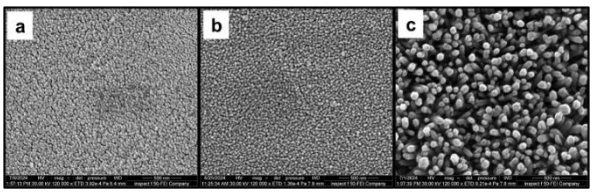

Figure 2. SEM images of ZnO nanowires after HWT treatment at 75°C on ITO substrate for (a) 10 min, (b) 20 min (c) 30 min

From Figure 2, the nanostructured ZnO films had a relatively rough, porous, nanorod-like morphology for all three samples. It can be clearly seen that the Zn film treated for 30 minutes showed more distinct, long and uniform nanorod-shaped nanostructures with diameters were ranging from 30-100 nm. The growth rate and orientation of ZnO NSs can be influenced by immersion time, and diffusion rates [13, 14].

3.1.1 Growth mechanism

ZnO nanostructure is produced using the catalyst-free HWT approach when Zn metal thin film samples are heated to 75°C. In summary, during HWT, a series of chemical interactions between metal atoms and water molecules result in the formation of metal oxide molecules. These molecules migrate in the water, and redeposition onto the metal surface to form Zinc oxide nanostructures. The formation details of zinc oxide nanostructures including plugging and surface diffusion mechanisms during hot water treatment method were investegated by Saadi et al. [10] and Smith et al. [13]. The water oxidizes Zn atoms during the HWT process as per the reaction given below [10, 15, 16]:

$$Zn^{+2} + OH^- \rightarrow Zn(OH)^+$$
$$Zn(OH)^{+} + OH^- \rightarrow Zn(OH)_2$$
$$Zn(OH)_2 \rightarrow ZnO + H_2O$$

Different parameters can effect the formation of nanostructure during HWT such as treatment time, amount of Oxygen dissolved, purity of water. However, the water's temperature during HWT is an essential factor in managing the growth of NSs [10].

Additionally, Smith et al. [13] looked at how temperature affected the morphological and structural characteristics of metal (aluminum) foil treated with hot deionized water at three distinct temperatures: 75°C, 85°C, and 95°C. According to their findings, the nanostructure grew more quickly at 95°C than at 75°C and 85°C. They proposed that the surface diffusion and plugging mechanisms during HWT accelerate the creation of nanostructures at high temperatures.

The previous experimental results reported by Al-Mayalee et al. [17] demonstrated that the metal thin film surface oxidizes much faster than metal sheets during HWT. This is can be due to the fact that a thick metal foils with polycrystalline structures need a long time to oxidize the different distributions of atomic planes densities depending on metal surface energy. In addition, the increasing number of surface defects in the nanostructured metal oxide films can accelerate the oxidation rate. The final shape, surface morphologies, and thickness of the synthesized metal oxide nanostructures are controlled by plugging and surface diffusion steps [10, 13].

3.2 Crystallographic analysis

Figure 3 displays the ZnO/ITO samples XRD diffraction pattern for different times of deposition. The synthesized zinc oxide nanostructures by HWT were validated by the distinct XRD peaks at 2θ angles linked to ZnO [1, 3-5, 18, 19].

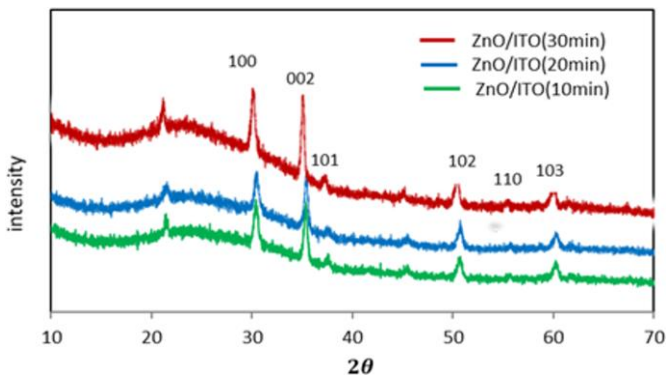

Figure 3. Show X-Ray diffraction of ZnO/ITO samples produced by HWT at various time at 75°C

As shown in Figure 3 for a growth time of 10 min, the characteristic XRD diffraction peaks of ZnO nanostructures are located at 2θ angles of 30.5◦ and 35.5◦, which correspond to the crystal planes of (100) and (002), respectively. After 20 minutes of hot water treatment, the XRD pattern of ZnO NSs showed the largest peaks at the 2θ values of 30.04◦ and 35.2◦, which corresponded to (100) and (002) planes. For the samples that were treated for 30 min, the largest peaks are observed at the 2θ values of 30° and 35° positions, which are assigned to the (100), (002) planes, respectively.

Table 1. The parameter of XRD- of ZnO/glass

HWT time	[2θ] deg	(d) nm	(hkl)	FWHM (β) rad	g (nm)
10min	30.5	0.293	100	0.009	15. 8
	35.5	0.253	2	0.0071	20.3
20min	30.1	0.297	100	0.0037	39
	35.2	0.255	2	0.006	23.8
30min	30	0.298	100	0.0015	94.5
	35	0.257	2	0.0012	118.9

Table 2. Structural properties of ZnO/glass for three times of HWT

HWT Time	2θ (deg) (100)	(a) Å (100)	g (nm)	2θ (deg) (002)	C (002) Å	g (nm)
10min	30.5	3.38	15.8	35.5	5.05	20.3
20min	30.04	3.39	39	35.2	5.09	23.8
30min	30	3.4	94.5	35	5.12	118.9

The parameter of XRD-diffraction showed in Table 1. The structural properties of all the samples are shown in Table 2. These findings are consistent with other research [1, 5, 7, 20-22] and show that the hexagonal wurtzite phase of the ZnO crystal is forming. The outcome is consistent with the literature (JCPDF card no. (36-1451) [1, 23]. The (101),)102), (110) and (103(peaks were also observed at 2θ = 36.8°, 49.6°, 54.4° and 60.6°, respectively yet compared to the (100),(002) peaks, these peaks are much less intense [3, 21, 22]. Using Scherrer's formula [24, 25], the average crystallite size of the most intense plane was calculated:

$$\frac{0.94\lambda}{\beta cos\theta} \quad (1)$$

where the wavelength of the x-ray is represented by λ (λ= 0.154056 nm), The degree of the XRD peaks' Bragg diffraction angle is indicated by θ, where β represents the (100) (002) diffraction peak's full width at half maximum (in radians), respectively. Around (14-42) nm is the approximate size of the crystallite. With longer processing times, results show that the crystallite size is rising. As the time of hot water treatment increases, the size of the nanostructures' crystallites increases can be attributed to a possible agglomeration of small crystallites to merge together and redeposited onto larger ones to become larger and more stable nanostructures with lower surface energy [10, 11]. On other word, the longer formation time allows for increased diffusion and coalescence process of smaller crystallites to occur [10, 17, 26].

The following relationships is used to get the values of the crystal lattice constants [25].

$$a = \sqrt{1/3}\frac{\lambda}{sin\theta} \quad (2)$$

$$c = \lambda/(sin\theta) \quad (3)$$

were λ the incident (Cu Kα) radiation's X-ray wavelength (λ=0.154056 nm).

The bulk ZnO from the JCPDS data with card number 36-1451 has pure lattice constants a and c of 3.2498 and 5.2066 Å, respectively.

3.3 Optical characterization

Figure 4 displays the UV-Vis absorption spectra of the ZnO nanorods produced using the HWT technique. For the investigation, optical absorption was measured using an ultraviolet-visible spectrometer in the wavelength range of (200-800) nm. As illustrated in Figure 4, the absorbance reduced with the increase of wavelength, and the ZnO nanorod structures transmit almost all of the visible spectrum energy. A shift of the absorption edge from 286 nm to 350 nm was observed of as-prepared ZnO nanorods at 75°C with growing times varying from 10, 20, and 30 minutes, these results agree with the findings of Foo et al. [25]. After the Zn thin films have been treated with hot water for 10 minutes, a weak and slightly broad absorption peak appears at 286 nm of 400 nm ZnO layer thickness. With increasing treatment time to 20 minutes, the absorbance for the 480 nm thickness of ZnO NSs becomes higher and border than that of 400 nm till 295 nm wavelength. The absorbance increases with increasing synthesize time to 30 minutes for the ZnO with thickness of 560 nm and the wavelength of the absorption edge changed to 350 nm. The observed displacements in the absorption edge to the higher wavelength (redshifts) are consistent with the observed variance in nanoparticle sizes, nature, and structure of ZnO nanorods, which have a high surface area with increasing HWT time.

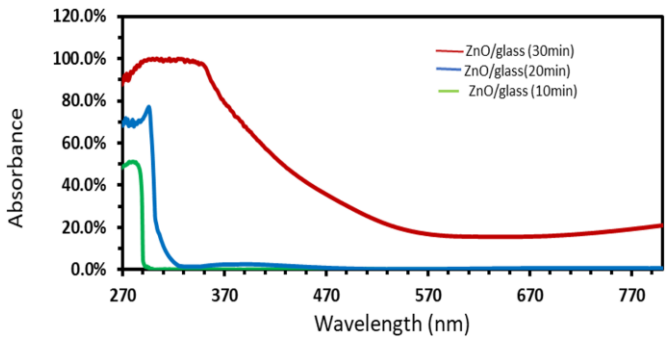

Figure 4. ZnO nanorods' absorption spectra on a glass substrate with varying growth times

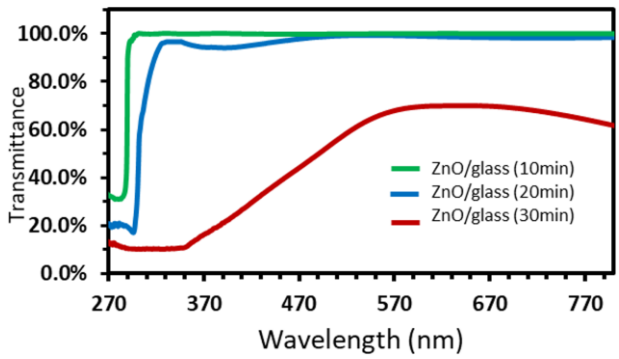

Figure 5. Transmittance spectra of ZnO nanorods by the HWT method for immersing times of 10, 20, 30 min

Figure 5 shows the transmittance spectra of ZnO nanorod samples. As can be seen, the transmittance spectra of the ZnO nanorod arrays decrease with decreasing wavelength and increasing hot water treatment time. The increasing of growth time leads to a decrease in transmittance from 95% at 10 min to almost 90% at 20 min and 48% at 30 min, This is explained by the thickening of the nanorod layer.

Eq. (4) is used for calculating the absorbance coefficient (α) of the ZnO nanorods transitional directions [1]:

$$\alpha = \frac{2.303A}{t} \tag{4}$$

while A is the ZnO film, s absorbance, t is the thickness of the films. The optical energy gap was calculated using these absorption coefficient values. Figure 6 explain $(\alpha h\nu)^2$ vs. hν, here hv is the incoming photon's energy and α is the spectral absorption coefficient. The energy gap (E_g), for direct linear transition between the valence and conduction bands, can be calculated using the following formula [25]:

$$\alpha h\nu = k\,(h\nu - E_g)^{1/2} \tag{5}$$

where hv is the energy of the incoming photon, E_g is the band gap, α is the absorbed energy coefficient, and k is the proportionality constant.

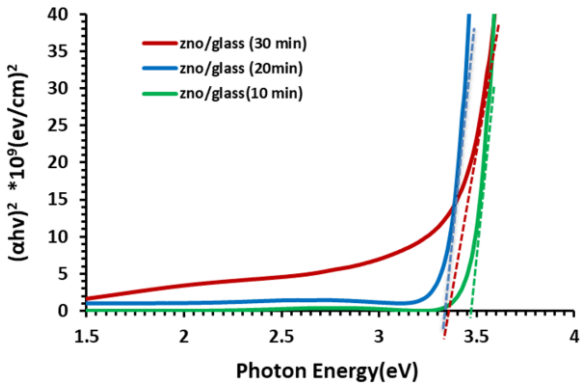

Figure 6. Energy band gap of ZnO/glass in different immersing time

The energy band gap E_g has been calculated from the intercept of the extrapolated linear portion of the curve, and it was found to be approximately 3.46 eV for ZnO NSs grown by HWT method at 75°C for 10 min, 3.35 eV for 20 min, and 3.32 eV for 30 min. The energy gap values of the grown films give a clear picture that the absorbance of these films found in the U-V region this finding is in excellent accordance with ZnO thin film data that has previously been published [21, 24]. Results indicated that the values of the energy gap reduced with increasing nanostructure synthesized time. This may be due to the increase in surface defects as HWT time increases, as a result, energy levels inside the ZnO gap arise and Eg shifts to lower values [2, 24, 25].

The following formulas may be used to compute the refractive index [1, 9, 25]:

$$\mathrm{n} = [N + (N2 - n_s^2)^{1/2}]1/2 \tag{6}$$

$$N = \frac{n_s^2 + 1}{2} + 2ns\frac{Tmax - Tmin}{TmaxTmin} \tag{7}$$

where ns is the substrate's refractive index. The transmittance spectrum's fitted envelope curves' optimum and lowest transmittances at the same wavelength are denoted by Tmax and Tmin. The refractive index curves of all thin films shown in Figure 7.

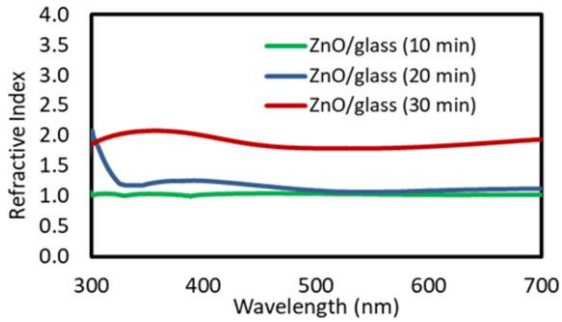

Figure 7. Refractive index curves of ZnO NSs

As shown in Figure 7, the deposited NSs through the hot water method have refractive index values ranging from 1.7 to 2, these values decrease with increasing wavelength. This variation is accompanied by a change in energy gap values, which are directly related to the deposition time and the increase in particle size, ultimately affecting the absorbance. Our refractive index values closely match the researcher's findings [1, 9].

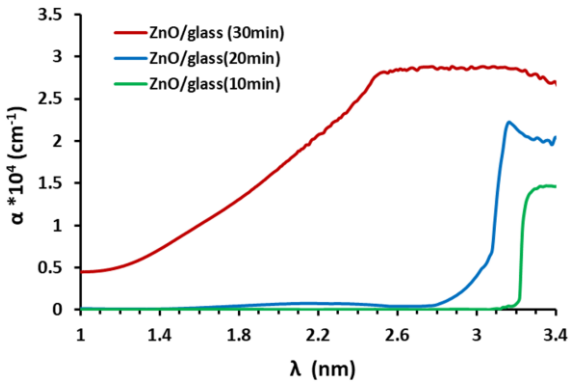

Figure 8. Absorption coefficient spectra of ZnO NSs in different time of HWT

The relationship $\alpha = (2.303\ A)/t$ was used to determine the optical absorption coefficient (α) of zinc oxide films treated with hot water for several durations (10, 20, 30 min). The absorption coefficient as a function of photon energy and hot water treatment duration is shown in Figure 8. It is shown in the graph that the electronic transfers are direct transfers as the absorption coefficient values are higher than (α 10^4 cm^{-1}), it is also clear that the absorption coefficient increases with increasing film treatment times as a result of the thin films' increased thickness and improved crystallinity. However, factors like thickness, surface morphology, and surface defects can contribute to the increased absorption of nanostructured materials [11, 17]. This result is similar to the result of research [1, 9].

4. CONCLUSIONS

In conclusion, zinc oxide nanostructures have been successfully produced on a glass substrate using an easy hot

water approach at 75°C for 10, 20 and 30 minutes. It has been investigated how time affects the rate of nanostructure growth. The films are all polycrystalline and in the hexagonal phase, according to the X-ray diffraction (XRD) investigation findings, and (100) and (002) are the optimum directions for crystal development. The results of the synthetic parameters indicated that the grain size rises with processing time. The optical findings demonstrated that the films exhibit excellent absorption at wavelengths in range 285nm - 300 nm, which decreases as wavelength increases as a consequence of the photon energy decreasing. It was also found that the ZnO samples that were treated in hot water for 10 and 20 min have high transmittance (> 90%) in the wavelength region (300-800) nm, while after 30 min of HWT it decreased to 48%. The index of refraction was computed and found to vary from 1.7 to 2. Results illustrated that the optical band gap of the synthesized nanostructures has been decreased with increasing deposition time and it is estimated to be 3.46, 3.35, and 3,32 eV for a hot water treatment time of 10 min, 20 min, and 30 min respectively. Our results indicated that the synthesize ZnO nanorod structures can used as transparent conducting oxides (TCOs) in many optoelectronics, including solar cells' windows. The controlled nanorod thickness, uniformity and high surface area of ZnO nanorods achieved during HWT can developed high efficiency solar cell and prompting a sustainable environment future.

ACKNOWLEDGMENTS

The researchers are grateful to Dr. Khaled Hanin and the College of Education for Girls, University of Kufa, for facilitating the completion of this research.

REFERENCES

[1] Amakali, T., Daniel, L.S., Uahengo, V., Dzade, N.Y., De Leeuw, N.H. (2020). Structural and optical properties of ZnO thin films prepared by molecular precursor and sol–gel methods. Crystals, 10(2): 132. https://doi.org/10.3390/cryst10020132

[2] Kim, H., Gilmore, C.M., Horwitz, J.S., Pique, A., et al. (2000). Transparent conducting aluminum-doped zinc oxide thin films for organic light-emitting devices. Applied Physics Letters, 76(3): 259-261. https://doi.org/10.1063/1.125740

[3] Tsoutsouva, M.G., Panagopoulos, C.N., Papadimitriou, D., Fasaki, I., Kompitsas, M. (2011). ZnO thin films prepared by pulsed laser deposition. Materials Science and Engineering: B, 176(6): 480-483. https://doi.org/10.1016/j.mseb.2010.03.059

[4] Moustaghfir, A., Tomasella, E., Amor, S.B., Jacquet, M., Cellier, J., Sauvage, T. (2003). Structural and optical studies of ZnO thin films deposited by rf magnetron sputtering: influence of annealing. Surface and Coatings Technology, 174: 193-196. https://doi.org/10.1016/S0257-8972(03)00417-1

[5] Hsu, Y.F., Xi, Y.Y., Djurišić, A.B., Chan, W.K. (2008). ZnO nanorods for solar cells: Hydrothermal growth versus vapor deposition. Applied Physics Letters, 92(13): 133507. https://doi.org/10.1063/1.2906370

[6] Morgan, J.H., Brodie, D.E. (1982). The preparation and some properties of transparent conducting ZnO for use in solar cells. Canadian journal of physics, 60(10): 1387-1390. https://doi.org/10.1139/p82-186

[7] Hasnidawani, J.N., Azlina, H.N., Norita, H., Bonnia, N.N., Ratim, S., Ali, E.S. (2016). Synthesis of ZnO nanostructures using sol-gel method. Procedia chemistry, 19: 211-216. https://doi.org/10.1016/j.proche.2016.03.095

[8] Ayouchi, R., Leinen, D., Martın, F., Gabas, M., Dalchiele, E., Ramos-Barrado, J.R. (2003). Preparation and characterization of transparent ZnO thin films obtained by spray pyrolysis. Thin Solid Films, 426(1-2): 68-77. https://doi.org/10.1016/S0040-6090(02)01331-7

[9] Ashour, A., Kaid, M.A., El-Sayed, N.Z., Ibrahim, A.A. (2006). Physical properties of ZnO thin films deposited by spray pyrolysis technique. Applied Surface Science, 252(22): 7844-7848. https://doi.org/10.1016/j.apsusc.2005.09.048

[10] Saadi, N.S., Hassan, L.B., Karabacak, T. (2017). Metal oxide nanostructures by a simple hot water treatment. Scientific Reports, 7(1): 7158. https://doi.org/10.1038/s41598-017-07783-8

[11] Al-Mayalee, K.H., Saadi, N., Badradeen, E., Watanabe, F., Karabacak, T. (2018). Optical and photoconductive response of CuO nanostructures grown by a simple hot-water treatment method. The Journal of Physical Chemistry C, 122(41): 23312-23320. https://doi.org/10.1021/acs.jpcc.8b06783

[12] Saadi, N., Alotaibi, K., Hassan, L., Smith, Q., Watanabe, F., Khan, A.A., Karabacak, T. (2021). Enhancing the antibacterial efficacy of aluminum foil by nanostructuring its surface using hot water treatment. Nanotechnology, 32(32): 325103. https://doi.org/10.1088/1361-6528/abfd59

[13] Smith, Q., Burnett, K., Saadi, N., Alotaibi, K., et al. (2021). Nanostructured antibacterial aluminum foil produced by hot water treatment against E. coli in meat. MRS Advances, 6: 695-700. https://doi.org/10.1557/s43580-021-00112-2

[14] Basher, M.K., Shah Riyadh, S.M., Hossain, M.K., Hassan, M., et al. (2023). Development of zinc-oxide nanorods on chemically etched zinc plates suitable for high-efficiency photovoltaics solar cells. Optical and Quantum Electronics, 55(4): 322. https://doi.org/10.1007/s11082-022-04474-1

[15] Saadi, N.S., Hassan, L.B., Sayem, S.M., More, K.L., Karabacak, T. (2024). Growth of zinc oxide nanowires by a hot water deposition method. Nanotechnology, 36(3): 035601. https://doi.org/10.1088/1361-6528/ad86c9

[16] Hariharalakshmanan, R.K., Martinez, J., Ergul-Yilmaz, B., Karabacak, T. (2023). Suspension of zno nanostructures synthesized by hot water treatment for photocatalytic wastewater treatment. Water, Air, & Soil Pollution, 234(4): 209. https://doi.org/10.1007/s11270-023-06192-0

[17] Al-Mayalee, K.H., Badraddin, E., Watanabe, F., Karabacak, T. (2019). CuO/Cu core/shell nanostructured photoconductive devices by hot water treatment and high pressure sputtering techniques. Nanotechnology, 31(9): 095204. https://doi.org/10.1088/1361-6528/ab5889

[18] Balela, M.D.L., Acedera, R.A., Flores, C.L.I., Pelicano, C.M.O. (2018). Surface modification of ZnO nanostructured film prepared by hot water oxidation. Surface and Coatings Technology, 340: 199-209.

https://doi.org/10.1016/j.surfcoat.2018.02.055
[19] Wibowo, A., Marsudi, M.A., Amal, M.I., Ananda, M.B., Stephanie, R., Ardy, H., Diguna, L.J. (2020). ZnO nanostructured materials for emerging solar cell applications. RSC Advances, 10(70): 42838-42859. https://doi.org/10.1039/D0RA07689A
[20] Choi, Y.S., Kang, J.W., Hwang, D.K., Park, S.J. (2009). Recent advances in ZnO-based light-emitting diodes. IEEE Transactions on Electron Devices, 57(1): 26-41. https://doi.org/10.1109/TED.2009.2033769
[21] Khedir, K.R., Saifaldeen, Z.S., Demirkan, T., Abdulrahman, R.B., Karabacak, T. (2017). Growth of zinc oxide nanorod and nanoflower structures by facile treatment of zinc thin films in boiling de-ionized water. Journal of Nanoscience and Nanotechnology, 17(7): 4842-4850. https://doi.org/10.1166/jnn.2017.13432
[22] Znaidi, L., Illia, G.S., Benyahia, S., Sanchez, C., Kanaev, A.V. (2003). Oriented ZnO thin films synthesis by sol–gel process for laser application. Thin Solid Films, 428(1-2): 257-262. https://doi.org/10.1016/S0040-6090(02)01219-1
[23] Sun, X.W., Ling, B., Zhao, J.L., Tan, S.T., et al. (2009). Ultraviolet emission from a ZnO rod homojunction light-emitting diode. Applied Physics Letters, 95(13): 133124. https://doi.org/10.1063/1.3243453
[24] Ahmed, N., Majid, A., Khan, M.A., Rashid, M., Umar, Z.A., Baig, M.A. (2018). Synthesis and characterization of Zn/ZnO microspheres on indented sites of silicon substrate. Materials Science-Poland, 36(3): 501-508. https://doi.org/10.2478/msp-2018-0058
[25] Foo, K.L., Hashim, U., Muhammad, K., Voon, C.H. (2014). Sol–gel synthesized zinc oxide nanorods and their structural and optical investigation for optoelectronic application. Nanoscale Research Letters, 9: 429. https://doi.org/10.1186/1556-276X-9-429
[26] Arunachalam, S., Balamurali, S., Suresh, R., Selvakumar, B., Sivaganesh, D. (2024). Facile synthesis of Mn doped ZnO for the sensing of ammonia. Chemical Physics Impact, 8, 100604. https://doi.org/10.1016/j.chphi.2024.100604